A NEW METHOD FOR AUTOMATIC MULTIPLE PARTIAL DISCHARGE CLASSIFICATION

L. Hao[1*], A. Contin[2], J. A. Hunter[1], P. L. Lewin[1], D. J. Swaffield[1], C. Walton[3] and M. Michel[4]
[1]Univerisity of Southampton, Southampton, UK
[2]University of Trieste, Trieste, Italy
[3]PPA Energy, Guildford, UK
[4]UK Power Networks, Crawley, UK
*Email: lh3@ecs.soton.ac.uk

Abstract: A new wavelet based feature parameter have been developed to represent the characteristics of PD activities, i.e. the wavelet decomposition energy of PD pulses measured from non-conventional ultra wide bandwidth PD sensors such as capacitive couplers (CC) or high frequency current transformers (HFCT). The generated feature vectors can contain different dimensions depending on the length of recorded pulses. These high dimensional feature vectors can then be processed using Principal Component Analysis (PCA) to map the data into a three dimensional space whilst the first three most significant components representing the feature vector are preserved. In the three dimensional mapped space, an automatic Density-Based Spatial Clustering of Applications with Noise (DBSCAN) algorithm is then applied to classify the data cluster(s) produced by the PCA. As the procedure is undertaken in a three dimensional space, the obtained clustering results can be easily assessed. The classified PD sub-data sets are then reconstructed in the time domain as phase-resolved patterns to facilitate PD source type identification. The proposed approach has been successfully applied to PD data measured from electrical machines and power cables where measurements were undertaken in different laboratories.

1 INTRODUCTION

Partial discharge (PD) classification and identification have been attracting a substantial amount of interest from researchers, utilities and manufacturers over the last few decades. Different PD classification features, rules, methods and knowledge bases have been developed based on different PD measurement systems. With the development of non-conventional wide bandwidth and ultra bandwidth PD sensors and high speed signal acquisition equipment, PD analysis tends to analyse the details of the PD pulse rather than the traditional time domain phase occurrence and amplitude based information only.

A large number of publications have reported promising results on PD classification or identification, however in most cases, the proposed approach only has been tested on a single PD source using particular equipment or laboratory experiment. In the case of multiple PD sources being activated simultaneously within power plant, the performance of the published methods are generally compromised or fail completely. To overcome such issues in PD source identification, different PD source classification/separation algorithms have been designed based on the analysis of PD pulses in time and frequency domain [1-3]. Phase resolved PD patterns and/or their statistical operators have been used as characteristics to classify different PD source types using machine learning techniques or fuzzy logic algorithms [3, 4].

In this paper, a new feature parameter i.e. the wavelet decomposition energy has been developed to represent the characteristics of PD activities. The wavelet decomposition energy is calculated using PD pulses measured from non-conventional ultra wide bandwidth PD sensors such as capacitive couplers (CC) or high frequency current transformers (HFCT). The generated feature vectors can contain different dimensions depending on the length of recorded pulses and decomposition level. The generated high dimensional feature vectors can then be processed using Principal Component Analysis (PCA) to map the data into a three dimensional space whilst the first three most significant components representing the feature vector are preserved. In the three dimensional mapped space, an automatic Density-Based Spatial Clustering of Applications with Noise (DBSCAN) algorithm is then applied to classify the data cluster(s) produced by the PCA. As the procedure is undertaken in three dimensional space, the obtained clustering results can be easily assessed. The classified PD data sets are then reconstructed in the time domain as phase-resolved patterns to facilitate PD source type identification. The proposed approach has been successfully applied to PD data measured from both electrical machines and power cables.

2 PD DATA ACQUISITION

PD data investigated in this paper were measured from HV cables and HV generators using different commercially available PD measurement equipment.

2.1 HV Cable PD data

The PD signal was measured using a split ferrite core High Frequency Current Transformer (HFCT) placed around the earth connection of HV cable, which has a bandwidth of 50 kHz – 20 MHz. The measured PD data were recorded using an Advanced Substation Monitor (ASM) which has been widely installed within the distribution network of UK Power Networks (UKPN).

PD phenomena within 11 kV three phase belted paper insulated lead cover (PILC) cable has been investigated in this paper. Both experimental data under controlled laboratory conditions and field on-line measurement data have been analyzed. The experiment for PD measurement is shown in Figure 1.

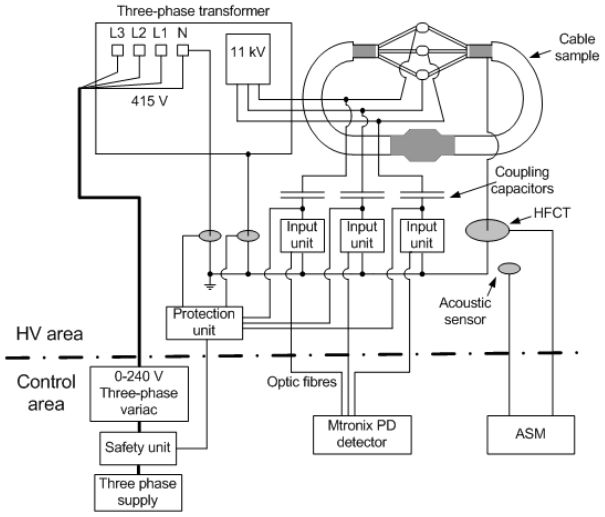

a.

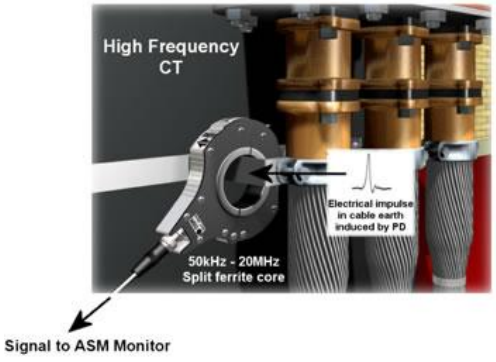

b.

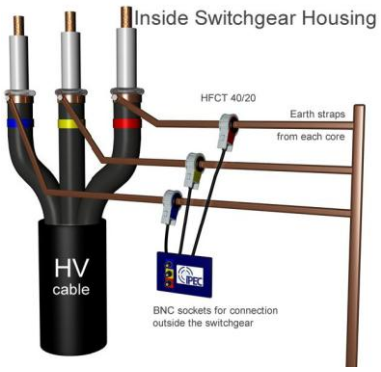

c.

Figure 1: Arrangement of PD measurement using ASM a. Schematic diagram of PD measurement in laboratory b. c. Field installations of HFCT [5]

As shown in Figure 1, the experiment is back-energized using a three-phase 11000/415 V delta/star distribution transformer. Three five-meter tails have been constructed using polymeric cables and terminals to connect between the HV side of the power transformer and the cable sample. The power transformer and polymeric cable tails have been tested and are PD free under rated conditions. In-line filters have been employed on the mains power supply in the control room and the resulting background noise level is 20 pC which is adequate for this investigation. Protection systems have been designed to protect the power supply under fault conditions and ensure safety of operators during operation [6]. The installation of PD sensors and ASM monitor in the field uses different arrangements as shown in Figure 1b and 1c [5].

The data acquisition unit within the ASM monitor samples across the power cycle at a sampling rate of 100 MS/s (50 MS/s for some old versions) with a 12bit resolution. The ASM monitor used in the laboratory experiment was connected to one HFCT and records one power cycle of data every 3 minutes. In the field, upto 128 PD sensors e.g. HFCT can be connected to the ASM monitor using multiplexers, therefore the recording interval between each acquisition for a particular sensor may be extended to 30 minutes. The obtained high resolution raw data were pre-processed to extract PD pulses and their phase occurrence.

In the laboratory controlled experiment, known defects has been inserted into a cable joint during the jointing process and act as an artificial PD source. The PD inception voltage was below rated voltage and PD measurements were taken under rated conditions.

2.2 Electrical machine PD data

In this case, the PD signal was generated from artificially defective conductor bars of ac rotating machines and accelerated aged induction motor coils. The signals were produced by known

sources under controlled conditions. PD measurements were performed using a digital waveform analyzer that records the complete time signature of signal pulses, using a sequence-mode technique. The instrumentation has a bandwidth of up to 200 MHz and operates at a suitable sampling rate (up to 500 MS/s) to avoid frequency aliasing. The measurement system is fully remotely-controllable by a personal computer. The waveform analyzer was connected to a 50 Ω resistor used as a measuring impedance. Different coupling capacitors were adopted in the tests using an indirect connection [7]. A low-pass filter (100 kHz cut-off frequency) was utilized to reject the low-frequency components of the test signal. The output of the acquisition process consists of a sequence of pulse signals along with their associated time pointers on the phase occurrence.

3 PD PULSE CHARACTERISATION AND CLASSIFICATION

3.1 Wavelet decomposition energy

The wavelet decomposition process works like a pair of complementary high-pass and low-pass filters, which decomposes the original signal into a series of detail and approximate coefficients respectively, as shown in Figure 2a, where S represents the original signal, D represents the detail decomposition coefficients and A represents the approximate decomposition coefficients. As an iterative process, the original signal can be decomposed into different levels, where each level is half the bandwidth (sampling rate in frequency domain) and half the length (sample number in time domain) than the above level, as shown in Figure 2b, where cA and cD represent the approximate and detail decomposition coefficients respectively and the number after cA or cD represents the decomposition level. Figure 3 shows an example of the decomposition coefficients at different levels.

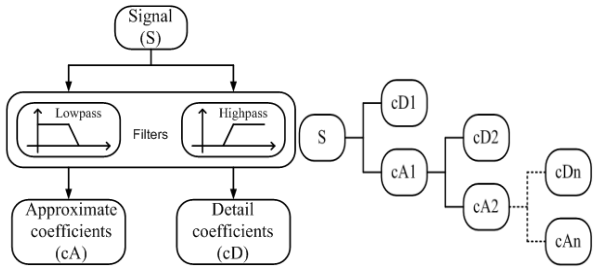

a. b.

Figure 2: Wavelet decomposition a. Complementary filters decomposition b. Iterative decomposition

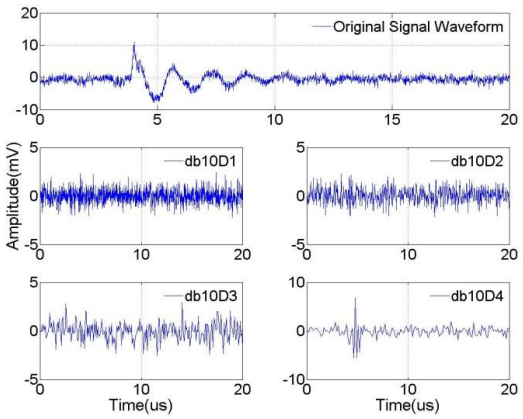

Figure 3: Wavelet decomposition coefficients

The energy of the coefficients at different decomposition levels can therefore be calculated using the following equations:

$$E_{Di} = \frac{\sum_{j=1}^{Nci} Cd_{i_j}^2(t)}{\sum_{i=1}^{n}\sum_{j=1}^{Nci} Cd_{i_j}^2(t) + \sum_{j=1}^{Ncn} Ca_n^2(t)} \cdot 100 \quad (1)$$

and

$$E_{An} = \frac{\sum_{j=1}^{Ncn} Ca_n^2(t)}{\sum_{i=1}^{n}\sum_{j=1}^{Nci} Cd_{i_j}^2(t) + \sum_{j=1}^{Ncn} Ca_n^2(t)} \cdot 100 \quad (2)$$

where E_{Di} is the energy of the detail decomposition coefficients, E_{An} is the energy of the approximate decomposition coefficients. *n* is the wavelet decomposition level. *Nc* is the number of decomposition coefficients. *Cd* and *Ca* are the detail and approximate decomposition coefficients respectively. The result obtained at each decomposition level using equations (5) and (6) is the percentage of the total signal energy. Therefore the produced feature vector consists of a set of values describing the percentage of total signal energy contained in each set of decomposition coefficients. The feature vector produced is then normalized to sum to 1. Figure 4 shows an example of the wavelet decomposition energy, expressed in terms of percentages.

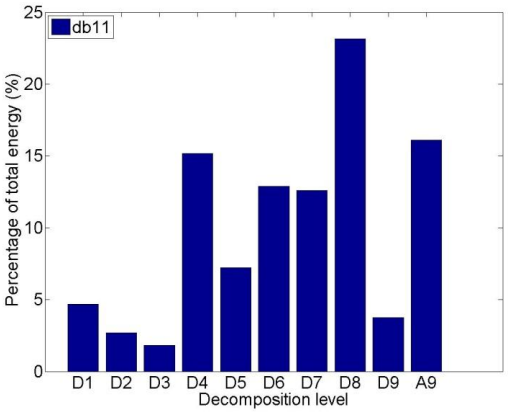

Figure 4: Wavelet decomposition energy

3.2 Principal Component Analysis

The wavelet energy based feature vector described above will have more than 3 dimensions, as the applied decomposition is more than 2 levels. Therefore it is impossible to represent the vector in a visible coordinate space, which must consist of no more than 3 dimensions. In order to visualise the wavelet energy vectors and manually verify the clustering and classification results, a dimension reduction technique has to be implemented to reduce the dimension of the feature vectors whilst preserving their characteristics.

Principal Component Analysis (PCA) is a non-parametric linear method that is extensively used for dimensionality reduction as well as simplifying the structure of complex data sets, by means of an orthogonal linear transformation in the direction of the greatest variance. PCA is applied here to reduce the number of energy levels associated to each decomposition level to three, thus allowing a representation of the PD signals in 3-D space.

The sample PD data sets (*X*) considered are expressed as *N* vectors, each comprising of M dimension columns (10 energy levels as the example shown in Figure 4), where *N* is the number of the pulse-like recorded signals. The PCA procedure is produced from solution of an eigenvalue problem that consists of: calculation of covariance matrix

$$\mathrm{cov}(X) = \frac{X \cdot X^T}{N-1} \quad (3)$$

Evaluation of eigenvalues (*λ*); mapping the input data to the new coordinate space using

$$P = v^T \times X \quad (4)$$

The mapped matrix represents the principal components with a decreasing significance. The first three components within the matrix are therefore plotted in a 3 dimensional space. Using this method, the recorded signals can be visually presented and the quality of the separation algorithm can also be manually verified.

3.3 Automatic clustering using Density Based Spatial Clustering of Applications with Noise

Among the various density-based clustering algorithms, DBSCAN has been considered for this application due to its ability to discover clusters of arbitrary shape as well as to distinguish noise (sparse points) in n-dimensional space. DBSCAN labels data points that are densely distributed and associated by a single cluster [8, 9]. Density represents the number of points, n, that fall in a small volume V surrounding a given point, P. V can be assumed as a hyper-sphere of radius ε centered at P, hence, the threshold density can be specified by a parameter n_{min} that represents the minimum number of points to make the volume V, significantly dense. ε and n_{min} are the two degrees of freedom defined by the method. Point P can either be a dense (core point) or non-dense point (non-core point). A non-dense point might be a border point of a dense region or disconnected (noise). In particular, as shown in Figure 5: A generic point Q, is a core-point if a number $n>n_{min}$ of points are included in the hyper-sphere V, having radius ε and centered at P; A point P is directly-density reachable (DDR) from Q if P is included in V and Q is a core-point; A point P is density reachable (DR) from R within V, if there is a chain of objects p_1, p_2…,p_n, where p_1=R and p_n=P, such that, for $1 \le i \le n$, $p_i \in Q$ and p_i+1 is DDR from p_i; A point S is density-connected (DC) to P in a set of volumes V_j, if there is an object $T \in V_j$ such that both S and P are DR from R.

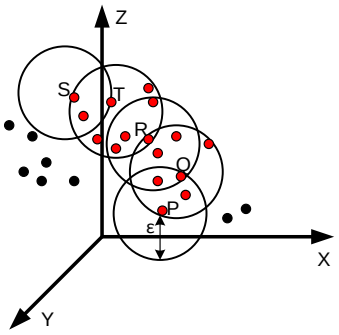

Figure 5: Principle of DBSCAN

A density-based cluster is defined as a set of density-connected points maximized with respect to the density-reachability concept. Every point not contained by a sufficiently populated cluster is classified as noise. Taking this into account, DBSCAN is a member of the partial clustering algorithm group. For any given ε, n_{min} value, by selecting an initial point P (randomly or resorting to the maximum/minimum weight of a selected function, e.g. considering the point that show the maximum frequency of occurrence), DBSCAN checks if P is a core-point. If this is found to be the case, it selects the DR and DDR points and expands the cluster by merging neighbouring dense regions together. Once the border of the first cluster is identified, DBSCAN selects another point P' in space that does not belong to a previously formed cluster and the procedure mentioned above is repeated [9]. The algorithm collects DDR from these core-points iteratively, which may involve the merging of a few density-reachable clusters. The process terminates when no new points can be added to any of the clusters.

4 RESULTS AND DISCUSSION

The proposed separation algorithm has been applied to analyze PD measurement results obtained testing a frame representing the complete stator coil of an HV induction motor rated at 11 kV.

The insulation system is based on mica tape impregnated with epoxy resin, completed with polyester-graphite tape and uses polyester-semiconductive tape as an end-winding corona suppression system. The stator coil was cured using vacuum pressure impregnantation (VPI) technology. The frame was subjected to an accelerated multi-factor aging procedure composed of a series of thermal, electrical and mechanical stresses. Each aging cycle had a duration of one week. PD patterns have been recorded before and after the aging process. A PD pattern was then recorded as shown in Figure 6.

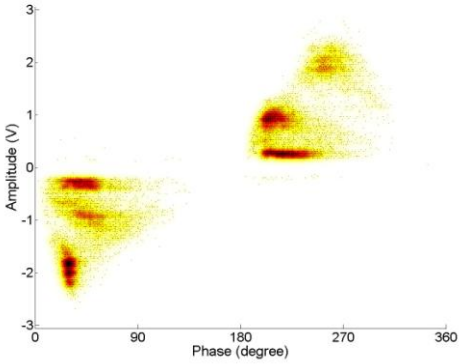

Figure 6: Phase resolved PD pattern obtained from coil of an induction motor at 6 kV after the inception of a new PD phenomenon

The automatic classification method proposed in section 3 has been applied to the obtained data. The clustering results are shown in Figure 7. The clustered PD pulses were then reconstructed using the phase resolved pattern, as shown in Figure 8.

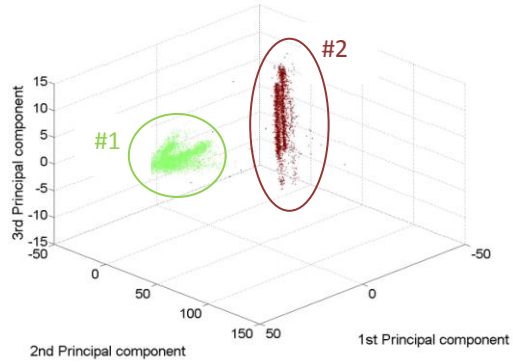

Figure 7: PCA and DBSCAN clustering result

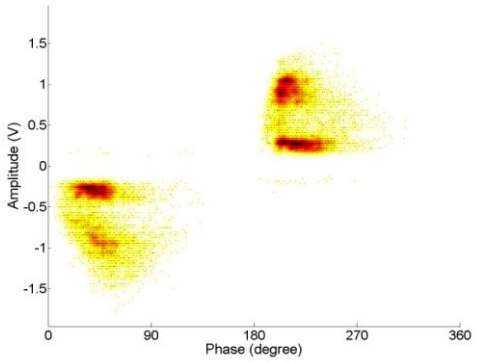

a.

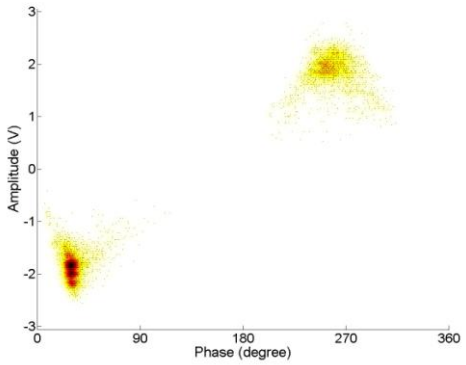

b.

Figure 8: Phase resolved pattern for each cluster a. cluster 1 b. cluster 2

Figure 8a shows typical pattern generated by distributed micro-voids within the coil sample. The new PD phenomenon due to tape delamination (macro-void) in the aging process has been shown in Figure 8b. This defect was confirmed after forensic analysis of the coil.

PD data obtained from the 11 kV PILC 3 phase cable utilized in a distribution network using the ASM monitor have also been analyzed. Figure 9 shows the pattern of 10 days of PD data.

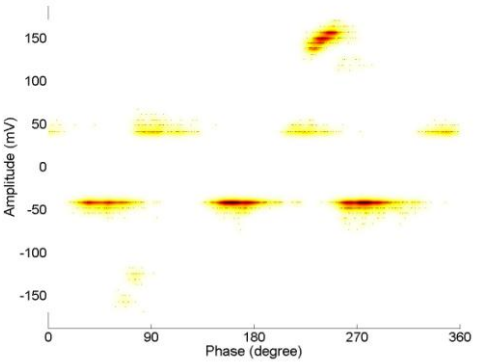

Figure 9: Phase resolved pattern of 326 power cycles

The measured PD pulses have been classified in to 2 clusters, as shown in Figure 10.

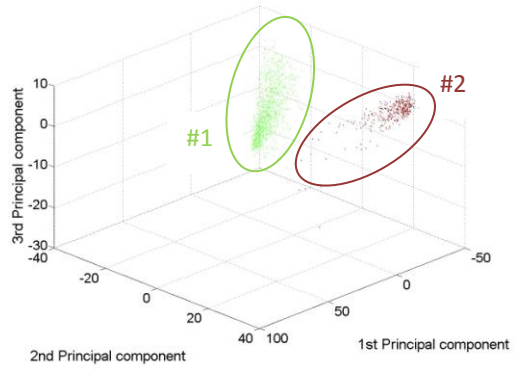

Figure 10: PCA and DBSCAN clustering result

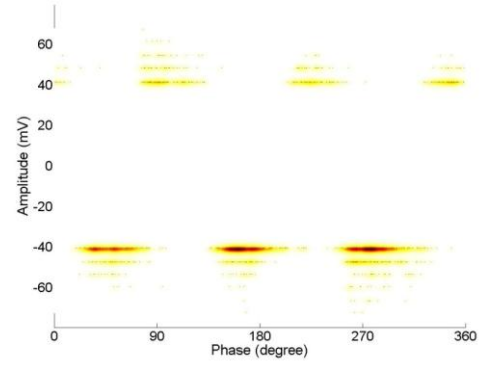

a.

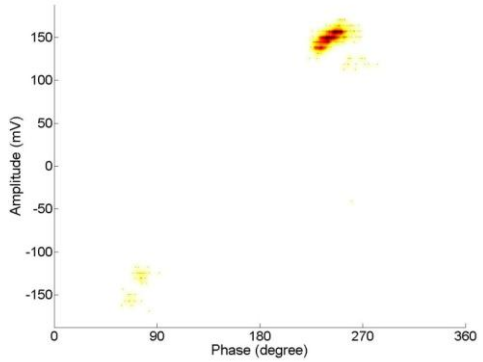

b.

Figure 11: Phase resolved pattern for each cluster a. cluster 1 b. cluster 2

Figure 11a represents a typical PD pattern produced by distributed voids which commonly exist within such mass-impregnated cable. Figure 11b shows the PD activity generated by a defect between the sheath and a phase conductor.

5 CONCLUSION

A new PD classification algorithm has been detailed in this paper. The method is based on the use of wavelet decomposition energy distribution as the feature vector; unsupervised learning i.e. Principal Component Analysis as the dimension reduction and feature extraction technique; and Density-Based Spatial Clustering of Applications with Noise as the automatic clustering technique.

The proposed method has been applied to analyze PD data measured from high voltage different plant. It has robust and effective performance in discriminating different PD sources. Moreover, the approach has shown an important advantage in term of minimizing the requirement from human intervention thus constituting a significant step forward in the development of automatic PD classification system.

6 ACKNOWLEDGMENTS

The financial and technical support of UK Power Networks for the work related to cable PD is gratefully acknowledged.

7 REFERENCES

[1] A. Cavallini, A. Contin, G. C. Montanari, F.Puletti, “Application of a New Methodology for Identification of PD in Electrical Apparatus”, IEEE TDEI, Vol. 12, No. 2, pp. 203-215, 2005

[2] A. Contin and S. Pastore, “Classification and Separation of Partial Discharge Signals by Means of their Auto-Correlation Function Evaluation”, IEEE TDEI, Vol. 16, No. 6, pp. 1609-1622, 2009

[3] L. Hao and P. L. Lewin, "Partial Discharge Source Discrimination using a Support Vector Machine", IEEE TDEI, Vol. 17, No. 1, pp. 189-197, 2010

[4] A. Contin, A. Cavallini, G. C. Montanari, G. Pasini, F. Puletti, “Digital Detection and Fuzzy Classification of Partial Discharge Signals”, IEEE TDEI, Vol. 9, pp. 335-348, 2002

[5] http://www.ipec.co.uk/asm/resources/assets/factsheets/ASM_On-line_PDM_Detailed_Overview_v2.0.pdf, last accessed: May 03, 2011

[6] J. A. Hunter, L. Hao, D. J. Swaffield, P. L. Lewin, N. Cornish, C. Walton and M. Michel, “Partial discharge in medium voltage three-phase cables”, IEEE ISEI, CD-ROM, 2010

[7] IEC 60270 Partial Discharge Measurements, 3rd Edition, 2001

[8] M. Ester, H. P. Kriegel, J. Sander and X. Xu, “A Density-Based Algorithm for Discovering Clusters in Large Spatial Databases with Noises”, Proc. 2nd Int. Conf. on Knowledge Discovery and Data Mining, pp. 226-231, 1996

[9] L. Kaufman and P. J. Rousseeuw, Finding Groups in Data: An Introduction to Cluster Analysis, New York, John Wiley & Sons, 1990